

Role of interaction with vinculin in recruitment of vinexins to focal adhesions

Honami Takahashi¹, Masaru Mitsushima¹, Naoya Okada, Takuya Ito, Sanae Aizawa, Rie Akahane, Tsutomu Umemoto, Kazumitsu Ueda, Noriyuki Kioka*

Division of Applied Life Sciences, Graduate School of Agriculture, Kyoto University, Sakyo-ku, Kyoto 606-8502, Japan

Received 29 July 2005

Available online 19 August 2005

Abstract

Although vinexin was originally identified as a protein binding to the proline-rich hinge region of vinculin, the functions and biochemical properties of the vinexin–vinculin interaction are not known. Here, we determined the affinity of the vinexin–vinculin interaction using surface plasmon resonance measurements and found that vinexin β interacts with the C-terminal half of vinculin, which mimics an activated “open” form, with a threefold higher affinity than with the full-length “closed” vinculin. Coimmunoprecipitation experiments showed that cell adhesion on fibronectin enhances the vinexin–vinculin interaction. We also show that the interaction with vinculin is necessary for the efficient localization of vinexin α and β at focal adhesions. These observations suggest a model that “activated” vinculin localized at focal adhesions recruits vinexins to focal adhesions.

© 2005 Elsevier Inc. All rights reserved.

Keywords: Vinculin; Vinexin; Actin cytoskeleton; SH3

Cell–extracellular matrix adhesion sites, also known as focal complexes or focal adhesions, play pivotal roles in regulating various aspects of cell behavior, including cell migration and cell proliferation [1–3]. Integrin cell adhesion receptors, as well as the termini of actin stress fibers and signaling and structural cytoplasmic molecules, are accumulated at focal adhesions. Vinexin is a cytoplasmic protein localized at focal adhesions [4–6], which is involved in regulating cell adhesion, cytoskeletal organization, and signal transduction. Vinexin is transcribed into at least two alternative forms, vinexin α and β [4,7]. Whereas vinexin α contains a sorbin homology (SoHo) domain at the N-terminus and three SH3 (src homology 3) domains at the C-terminus, vinexin β has only the three SH3 domains. Vinexin α belongs to a novel family of adaptor proteins, including ArgBP2 and c-cbl associated protein/ponsin, all

of which have a SoHo domain and three SH3 domains [4,8–12]. Both vinexin α and β are located at focal adhesions, but only vinexin α efficiently induces the accumulation of F-actin at focal adhesions and the formation of actin stress fibers in NIH3T3 cells [4]. Furthermore, the exogenous expression of vinexin β allows anchorage-independent ERK2 activation stimulated by epidermal growth factors [13].

Vinculin is another cytoplasmic protein localized at focal adhesions, which is known to bind to vinexin. Vinculin is composed of a “head” domain and a “tail” domain, as well as a proline-rich hinge region [2,14,15]. The head domain binds to other actin-binding proteins, talin and α -actinin, whereas the tail domain binds to F-actin and paxillin. Intramolecular interaction of the head and tail domains inhibits its phosphorylation [2,14] and its ability to bind to target proteins [16–20]. The binding of phosphatidylinositol-4,5-bisphosphate to the tail domains inhibits this intramolecular association, exposing binding sites for target proteins [21–23]. In addition, we and others found that

* Corresponding author. Fax: +81 75 753 6104.

E-mail address: nkioka@kais.kyoto-u.ac.jp (N. Kioka).

¹ These authors contributed equally to this work.

the proline-rich hinge region also functions as a protein-binding domain for actin-regulating proteins, including vinexin, ponsin, vasodilator-stimulated phosphoprotein (VASP), and Arp2/3 [4,11,24–26]. Recent structural analyses have revealed that the vinculin tail domain is held pincer-like by subdomains of the head region and that the binding affinity for target proteins is regulated sterically and allosterically [27–30]. Exogenous expression of vinculin enhances cell attachment to the extracellular matrix, cell spreading, and actin stress fiber formation, but inhibits cell migration [31,32]. In contrast, gene disruption of vinculin inhibits cell adhesion and affects the cytoskeletal organization, but stimulates cell motility [33–37]. Furthermore, reduced expression of vinculin allowed cells to survive and proliferate in an anchorage-independent manner [37–39]. Thus, vinculin plays a pivotal role in regulating the formation of the actin cytoskeleton, cell adhesion, and cell adhesion-induced signaling.

Both vinexin and vinculin play roles in regulating cell adhesion, the cytoskeletal organization, and adhesion-induced signaling. However, the functions of the vinexin–vinculin interaction through the proline-rich hinge region of vinculin are unclear. Here, we determined the affinity of the vinexin–vinculin interaction and found that vinexin β interacts with higher affinity with the C-terminal half of vinculin than the full-length vinculin. We also provide evidence that this interaction is necessary for the efficient localization of vinexins at focal adhesions. These observations suggest a model that “activated” vinculin localized at focal adhesions recruits vinexins to focal adhesions.

Materials and methods

Plasmids. Plasmids for GFP-tagged vinexin α and β , and point mutants mutated in each SH3 domain (α 1stWF, α 2ndWF, α 3rdWF, β 1stWF, β 2ndWF, and β 3rdWF) were constructed from the plasmids encoding the FLAG-tagged mutants [4,5,13] using restriction enzymes. The expression plasmid for GFP-tagged full-length chick vinculin was a generous gift from Dr. B. Geiger and Dr. S. Aota. To express the GST-tagged C-terminal half of vinculin in *Escherichia coli*, a plasmid containing the proline-rich hinge region and tail region (amino acids 836–1066) of chick vinculin, pRG425 (a gift from Dr. S. Aota), was subcloned into pGEX4T-1 (Amersham Pharmacia Biotech). To express histidine and thioredoxin (HisTrx)-tagged vinexin β , full-length vinexin β was subcloned into pET32a (Novagen).

Surface plasmon resonance. HisTrx-tagged vinexin β and mutants of vinexin β were expressed and purified as described previously [4]. Full-length vinculin was purified from chick gizzard as reported [40]. The GST-tagged C-terminal half of vinculin was purified as described previously [4] and the GST tag was removed by thrombin (Amersham Biosciences) according to the manufacturer's instructions. Surface plasmon resonance (SPR) analyses were performed using a BIACORE 2000 instrument (BIACORE, Uppsala, Sweden). In all experiments, HBS (10 mM Hepes (pH 7.4), 150 mM NaCl, 3 mM EDTA, and 0.005% Surfactant P20) was used as running buffer. Typically, 200–500 resonance units (RU) of purified protein was coupled to F1 sensor chips (BIACORE) according to the manufacturer's instructions. Vinexin and vinexin mutants were then tested for binding and dissociation using a flow rate of 20 μ l/min. The K_d values were calculated using the BIAevaluation 3.0 software (BIACORE) in the context of a first-order kinetic model ($A + B \rightleftharpoons AB$) and shown as an average of at least three independent experiments.

Immunoprecipitation. To detect the interaction of vinexin β or vinexin β mutants with vinculin, FLAG-tagged vinexin β and its mutants were transfected into COS-7 cells with GFP-tagged vinculin. Cells were then lysed and immunoprecipitated with anti-FLAG M2 antibody as described previously [41]. The bound proteins were detected using anti-GFP antibody or anti-vinculin antibody VII-F9 (a gift from Dr. V. Koteliansky).

Immunostaining. NIH3T3 or vinculin-null mouse fibroblast cells (gifts from Dr. E. Adamson) were plated on coverslips 24 h after transfection of the expression plasmids using LipofectAMINE Plus (Invitrogen). After a further 24 h incubation, the cells were fixed as described previously [4]. For the staining of F-actin, rhodamine–phalloidin (Molecular Probes) was used. Fluorescence micrographs were obtained using an Axiovert microscope (Carl Zeiss) equipped with a MicroRadiance Confocal Laser Scanning microscope (Bio-Rad Laboratories) or Olympus IX51. To quantitate the effects of vinexin α on F-actin, wild-type and SH3 mutants of vinexin α tagged with FLAG were cotransfected with GFP into NIH3T3 cells, and the distribution of F-actin in GFP-expressing cells was estimated. For each slide, at least 20 cells with GFP fluorescent signals were classified as having stress fibers with normal ends or swollen ends, or having no stress fibers. Scoring was done blind to which construct was being analyzed. Each construct was analyzed using two separate transfections.

Results and discussion

Interaction of vinexin β with vinculin *in vitro* and *in vivo*

Exogenous expression of either vinexin or vinculin enhanced the actin cytoskeletal organization. It raised the possibility that the interaction between vinexin and vinculin is important in regulating the formation of actin cytoskeleton. To better understand the interaction between vinexin and vinculin, we examined the real-time binding of vinexin β and its mutants (Fig. 1A) to full-length vinculin purified from chick gizzards using SPR measurements. As shown in Fig. 1B, HisTrx-tagged vinexin β purified from an *E. coli* expression system clearly showed an association with and dissociation from the vinculin immobilized on the sensor chip. The dissociation constant (K_d) calculated from the data was $(3.7 \pm 0.4) \times 10^{-7}$ M. HisTrx alone did not show any significant association with vinculin (data not shown). Furthermore, a point mutation (substitution of the conserved tryptophan residue in each SH3 domain with phenylalanine) either in the first or second SH3 domain of vinexin β (β 1stWF and β 2ndWF) completely disrupted this interaction (Fig. 1C). In contrast, vinexin β having a point mutation in the third SH3 domain (β 3rdWF) interacted with vinculin with similar affinity ($K_d = (5.0 \pm 1.6) \times 10^{-7}$ M) to wild-type vinexin β . Vinexin α was highly degraded when expressed in *E. coli*, thus we could not examine its affinity for vinculin. These observations suggest that vinexin β directly associates with vinculin and the association requires both the first and second SH3 domains.

It has been shown that intramolecular interaction between the head and tail domains of vinculin regulates its ability to bind to target proteins, such as talin, actin, and VASP [21–23]. Thus, we examined whether the affinity of vinexin β for vinculin is also regulated by the intramolecular

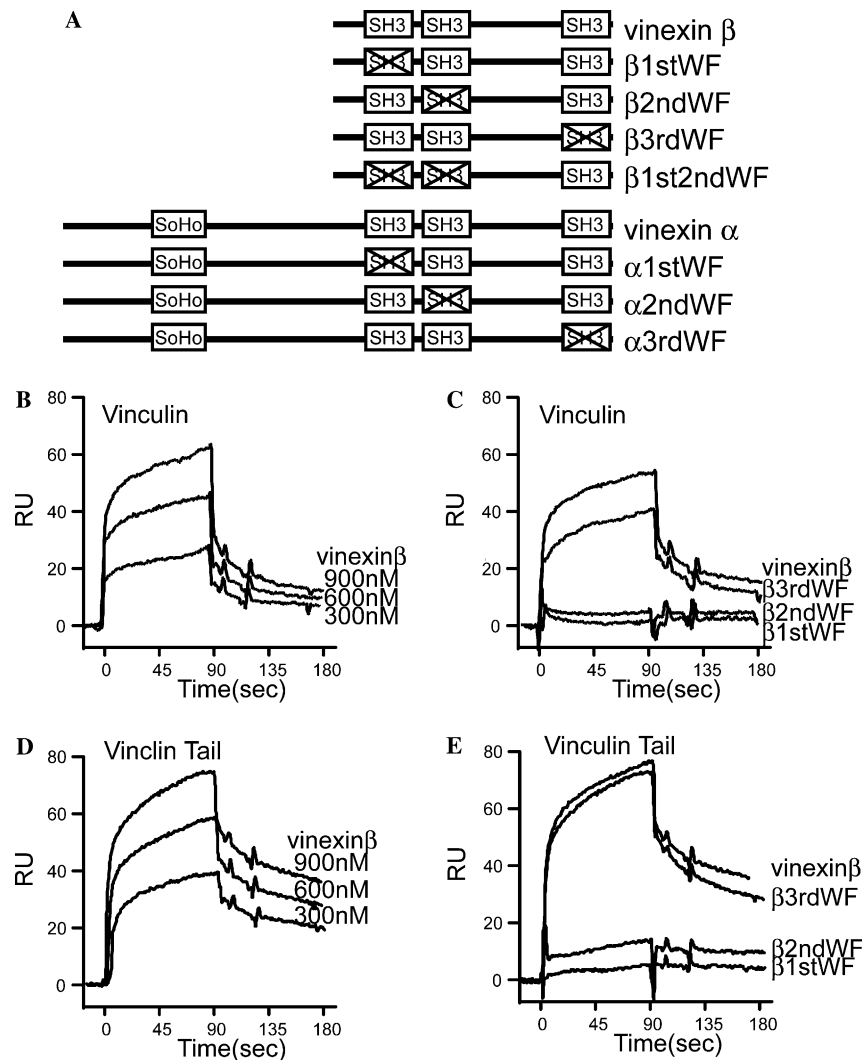


Fig. 1. Sensorgrams of the association phase and dissociation phase for binding of vinexin β and its SH3 mutants to full-length and C-terminal half of vinculin. (A) A schematic diagram of the vinexin mutants used in this study. (B–E) Full-length vinculin (B,C) or the C-terminal half of vinculin (D,E) was immobilized on the F1 sensor chip and probed with the indicated concentration of wild-type HisTrx-vinexin β (B,D) or 900 nM of HisTrx-vinexin β and its mutants (C,E) at a flow rate of 20 μ l/min, as described under Materials and methods. The results are representative of at least three independent experiments.

interaction of vinculin. SPR analyses showed that the binding affinity of vinexin β for the C-terminal half of vinculin, which contains the proline-rich hinge region and tail domain and is thought to mimic an activated “open” form [16–18], is three times higher ($K_d = (1.1 \pm 0.1) \times 10^{-7}$ M) than that for full-length vinculin. As was the case with full-length vinculin, β 3rdWF associated with the C-terminal half of vinculin with similar affinity ($K_d = (1.4 \pm 0.1) \times 10^{-7}$ M) to wild-type vinexin β , but β 1stWF or β 2ndWF did not associate. Together, these results suggest that the interaction is regulated by the intramolecular interaction of vinculin. Recently, our collaborator reported that interaction of vinculin with IpaA increased the affinity to vinexin β [42]. Their report is consistent with our study, since the interaction of vinculin with IpaA is known to change the activation status of vinculin.

Vinculin is reported to be an inactive “closed” form in the cytosol and to be changed to an active “open” form at focal adhesions [27,29,42]. Thus, we examined the vinexin–vinculin interaction in adherent and suspended conditions to confirm that vinexin associates with activated vinculin in vivo. NIH3T3 cells were trypsinized and maintained in suspension for 3 h. Cells were then reattached on fibronectin or kept in suspension for further 2 h. Cell lysates were immunoprecipitated with anti-vinexin antibody and co-precipitated vinculin was determined (Fig. 2). Endogenously expressed vinculin was co-precipitated with vinexin in adherent cells but not in suspended cells. Rabbit IgG did not precipitate either vinexin or vinculin even in adherent cells. These results support the idea that the interaction is regulated by the intramolecular interaction of vinculin in vivo.

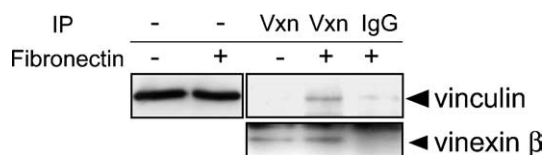


Fig. 2. Co-immunoprecipitation of endogenous vinculin with vinexin. NIH3T3 cells were trypsinized and maintained in suspension for 3 h. Cells were then reattached on fibronectin or kept in suspension for further 2 h. Cells were lysed and cell lysates were immunoprecipitated with anti-vinexin antibody. Co-precipitated vinculin was detected by immunoblotting. The results are representative of three independent experiments.

Role of interaction with vinculin in recruitment of vinexins to focal adhesions

To determine the function of vinexin–vinculin interaction in vivo, we first confirmed the interaction of vinexin with vinculin through its first and second SH3 domains. GFP-tagged vinculin was transfected with FLAG-tagged wild-type or SH3 mutants of vinexin β into Cos7 cells. Cell lysates were then immunoprecipitated with anti-FLAG antibody. As shown in Fig. 3A, GFP-vinculin as well as

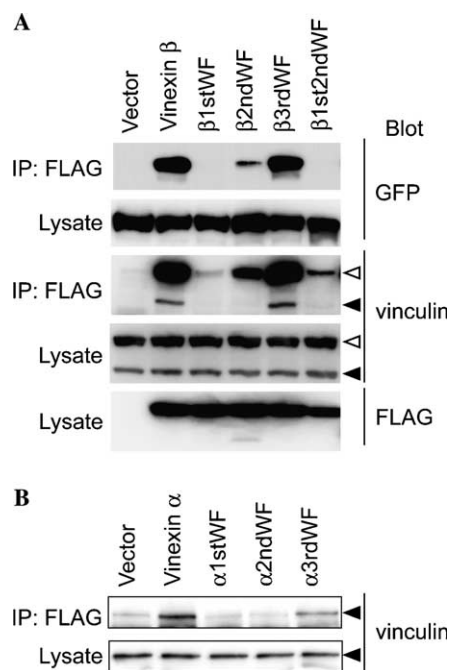


Fig. 3. In vivo association of vinexin β through its first and second SH3 domains with vinculin. (A) COS-7 cells were transfected with vector alone or FLAG-tagged vinexin β or SH3 mutants with GFP-tagged vinculin. Cell lysates were immunoprecipitated (IP) with anti-FLAG antibody. Immunocomplexes were subjected to immunoblotting using anti-GFP antibody or anti-vinculin antibody to detect co-precipitated vinculin. Cell lysates were immunoblotted using anti-GFP antibody or anti-vinculin antibody to confirm the equal expression of vinculin. White arrowheads show GFP-vinculin and black arrowheads show endogenous vinculin. (B) COS-7 cells were transfected with vector alone or FLAG-tagged vinexin α or its SH3 mutants. Cell lysates were immunoprecipitated (IP) with anti-FLAG antibody and immunoblotted using anti-vinculin antibody as described in (A). The results are representative of three independent experiments.

endogenous vinculin was coimmunoprecipitated with wild-type vinexin β and the β 3rdWF mutant. In contrast, GFP-vinculin and endogenous vinculin were barely coimmunoprecipitated with β 1stWF, β 2ndWF, or β 1st2ndWF. We also confirmed the interaction of vinexin α with vinculin. As in the case of vinexin β , vinculin was significantly coimmunoprecipitated with wild-type vinexin α and the mutant α 3rdWF, but not with α 1stWF or α 2ndWF (Fig. 3B). Less vinculin was coimmunoprecipitated with vinexin α than with vinexin β possibly due to the much lower solubility of vinexin α (data not shown). These observations are consistent with the results obtained by SPR that vinexin associates with vinculin through its first and second SH3 domains.

To determine the role of binding in the subcellular distribution of vinexin β , GFP-tagged vinexin β or its SH3 mutants was transfected into NIH3T3 cells. The subcellular localization of vinexin β was observed as GFP fluorescence. Wild-type vinexin β was predominantly localized at focal adhesions and co-localized with vinculin (Fig. 4A) as previously described [4]. A mutation in the third SH3 domain of vinexin β did not affect the subcellular localization (Fig. 4D). In contrast, β 1stWF and β 2ndWF showed a diffuse subcellular distribution with little accumulation at focal adhesions (Figs. 4B and C). These results suggested that the interaction with vinculin through the first and second SH3 domains is required for the localization of vinexin β at focal adhesions.

We next determined the subcellular distribution of GFP-tagged vinexin α and SH3 mutants in NIH3T3 cells. Wild-type vinexin α and α 3rdWF were predominantly localized at focal adhesions. In contrast, α 1stWF and α 2ndWF showed a more diffuse distribution, although a portion of these mutants were still localized at focal adhesions and colocalized with vinculin (see Fig. 6 and data not shown). This localization may be mediated by another focal adhesion-localizing signal included in the N-terminal half of vinexin α [4] and/or by a weak association of these mutants with vinculin through remaining functional SH3 domains. To confirm the importance of vinculin for localization of vinexins at focal adhesions, we determined the localization of vinexin α and β in vinculin-null fibroblasts (Fig. 5). Both vinexin α and β were clearly co-localized with paxillin at focal adhesions in wild-type fibroblasts. In contrast, vinexin β showed a diffused subcellular distribution in vinculin-null fibroblasts as we expected. Furthermore, vinexin α showed a diffuse and fibrillar distribution where paxillin was not localized, with slight accumulation at focal adhesions in vinculin-null fibroblasts. Together, these results suggested that interaction with vinculin plays an important role in the recruitment of vinexin α and β to focal adhesions. Furthermore, our observations also indicate that vinexin α can localize at fibrillar structures and less efficiently at focal adhesions in a vinculin-independent manner.

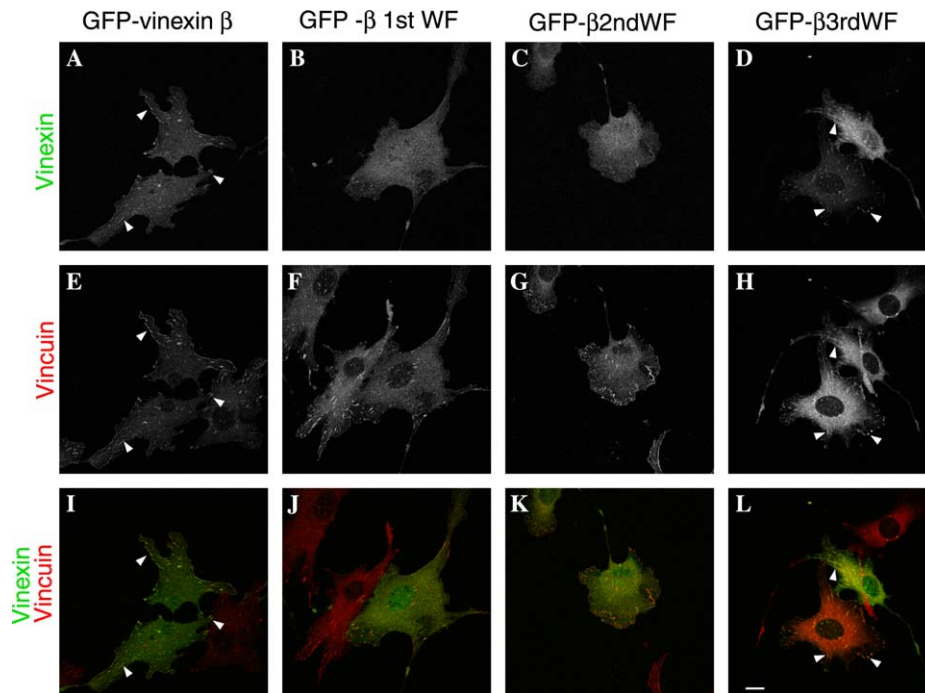


Fig. 4. Subcellular localization of vinexin β . GFP-tagged vinexin β (A,E,I), β 1stWF (B,F,J), β 2ndWF (C,G,K), and β 3rdWF (D,H,L) were each transfected into NIH3T3 cells. Transfected cells were examined for GFP fluorescence (A–D) and indirect immunofluorescence labeling for vinculin (E–H). Merged images of GFP fluorescence (green) and vinculin staining (red) are also shown (I–L). Arrowheads indicate the sites of colocalization of vinexin β with vinculin. The scale bar indicates 10 μ m. The results are representative of at least three independent experiments. (For interpretation of the references to color in this figure legend, the reader is referred to the web version of this paper.)

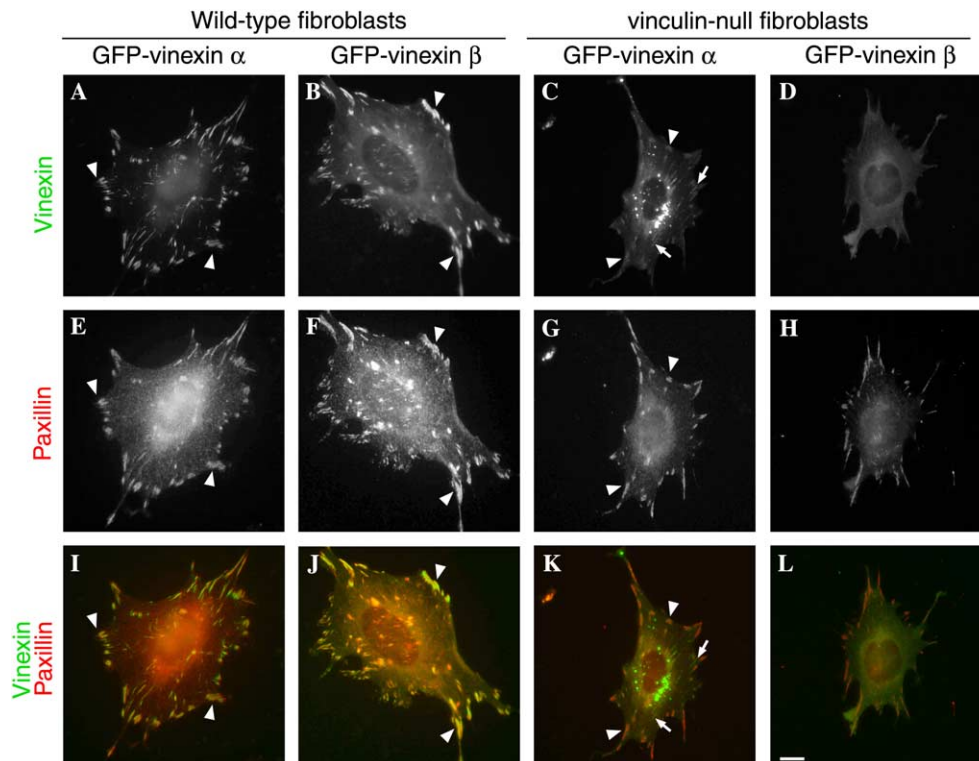


Fig. 5. Subcellular localization of vinexin α and β in wild-type and vinculin-null fibroblasts. GFP-tagged vinexin α (A,C,E,G,I,K) or β (B,D,F,H,J,L) was transfected into wild-type (A,B,E,F,I,J) or vinculin-null fibroblasts (C,D,G,H,K,L). Transfected cells were examined for GFP fluorescence (A–D) and indirect immunofluorescence labeling for paxillin using anti-paxillin mAb (Transduction Laboratories) (E–H). Merged images of GFP fluorescence (green) and paxillin staining (red) are also shown (I–L). Arrowheads indicate the sites of colocalization of vinexins with paxillin. Arrows indicate the sites of fibrillar localization of vinexin α where paxillin was not localized. The scale bar indicates 10 μ m. The results are representative of at least three independent experiments. (For interpretation of the references to color in this figure legend, the reader is referred to the web version of this paper.)

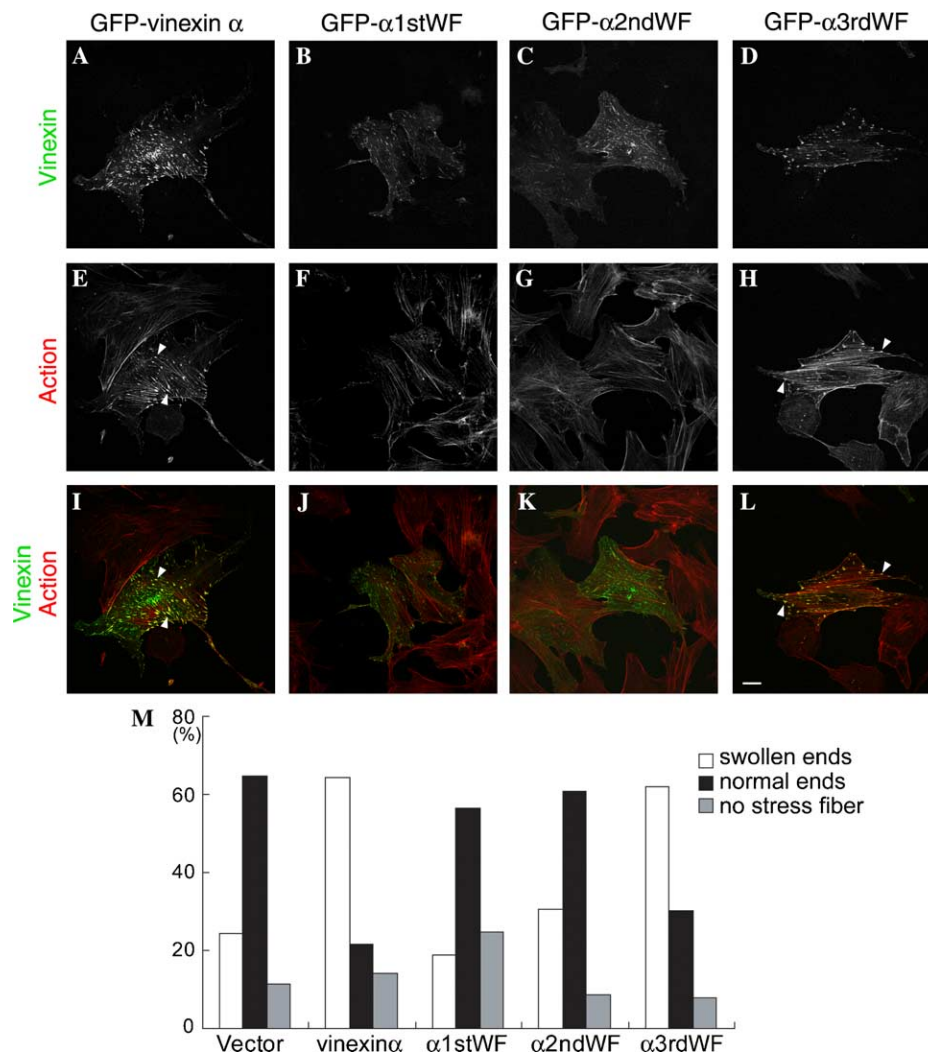


Fig. 6. Confocal microscopic images of cells expressing vinexin α and its mutants. GFP-tagged vinexin α (A,E,I), α 1stWF (B,F,J), α 2ndWF (C,G,K), and α 3rdWF (D,H,L) were each transfected into NIH3T3 cells. Transfected cells were examined for GFP fluorescence (A–D), rhodamine-phalloidin (E–H), and overlaid GFP and rhodamine fluorescence (I–L). Arrowheads show enhanced rhodamine–phalloidin staining in the vinexin α -expressing cells. The scale bar indicates 10 μ m. The results are representative of at least three independent experiments. (M) Quantitation of the effects of vinexin α on stress fibers. FLAG-tagged vinexin α or SH3 mutants were cotransfected with GFP into NIH3T3 cells, and the distribution of F-actin in GFP-expressing cells was estimated by immunofluorescence microscopy. Scoring was done blind to which construct was being analyzed. Each construct was analyzed using two separate transfections. The ordinate indicates the percentage of cells having stress fibers with swollen ends or normal ends, or having no stress fibers.

Vinculin-binding region is required for vinexin α to induce the accumulation of F-actin at focal adhesions

We previously showed that the exogenous expression of vinexin α in NIH3T3 cells induced the accumulation of F-actin at focal adhesions [4]. To examine the importance of the vinculin-binding region in this effect, NIH3T3 cells were transfected with GFP-tagged vinexin α or GFP-tagged SH3 mutants of vinexin α and stained with rhodamine-labeled phalloidin (Fig. 6). Expression of wild-type vinexin α as well as α 3rdWF efficiently induced the accumulation of F-actin at focal adhesions, i.e., the swollen ends of stress fibers (Figs. 6E and H). In contrast, α 1stWF and α 2ndWF only slightly affected the actin organization (Figs. 6F and G). To quantitate these effects, FLAG-tagged vinexin α and the mutants were cotransfected with

GFP into NIH3T3 cells, and the distribution of F-actin in GFP-expressing cells was estimated. Less than 30% of cells transfected with vector alone ($n = 62$), α 1stWF ($n = 53$), or α 2ndWF ($n = 46$) contained swollen ends of stress fibers (Fig. 6M). In contrast, 64% ($n = 56$) and 62% ($n = 63$) of cells expressing wild-type vinexin α and α 3rdWF, respectively, had swollen ends of stress fibers. Together, these observations suggested that the interaction with vinculin through the first and second SH3 domains of vinexin α is involved in inducing the accumulation of F-actin at focal adhesions, although we cannot exclude a possibility that other vinexin-binding proteins may be involved in this phenomenon.

In conclusion, our data suggest that the interaction of vinexin with vinculin through its first and second SH3 domains is necessary for efficient localization of vinexin α and

β at focal adhesions. We also observed that vinexin β interacts with higher affinity with the C-terminal half of vinculin, which mimics an activated “open” form, than with full-length vinculin and vinculin was co-precipitated with vinexin in adherent cells but not in suspended cells. Full-length vinculin is thought to be an inactive “closed” form in the cytosol and to be changed to an active “open” form at focal adhesions [27,29,42]. We, therefore, propose the model that activated vinculin localized at focal adhesions recruits vinexins to focal adhesions.

Acknowledgments

We thank Drs. E. Adamson, V. Kotliansky, B. Geiger, and S. Aota for providing valuable materials. This work was supported in part by The Asahi Glass Foundation, The Naito Foundation, and a Grant-in-Aid for Scientific Research from the Ministry of Education, Culture, Sports, Science and Technology of Japan.

References

- [1] E. Zamir, B. Geiger, Molecular complexity and dynamics of cell-matrix adhesions, *J. Cell Sci.* 114 (2001) 3583–3590.
- [2] D.R. Critchley, Focal adhesions—the cytoskeletal connection, *Curr. Opin. Cell Biol.* 12 (2000) 133–139.
- [3] R.O. Hynes, Integrins: bidirectional, allosteric signaling machines, *Cell* 110 (2002) 673–687.
- [4] N. Kioka et al., Vinexin: a novel vinculin-binding protein with multiple SH3 domains enhances actin cytoskeletal organization, *J. Cell Biol.* 144 (1999) 59–69.
- [5] M. Akamatsu, S. Aota, A. Suwa, K. Ueda, T. Amachi, K.M. Yamada, S.K. Akiyama, N. Kioka, Vinexin forms a signaling complex with Sos and modulates epidermal growth factor-induced c-Jun N-terminal kinase/stress-activated protein kinase activities, *J. Biol. Chem.* 274 (1999) 35933–35937.
- [6] M. Mitsushima, A. Suwa, T. Amachi, K. Ueda, N. Kioka, Extracellular signal-regulated kinase activated by epidermal growth factor and cell adhesion interacts with and phosphorylates vinexin, *J. Biol. Chem.* 279 (2004) 34570–34577.
- [7] T. Kawauchi, M. Ikeya, S. Takada, K. Ueda, M. Shirai, Y. Takihara, N. Kioka, T. Amachi, Expression of vinexin alpha in the dorsal half of the eye and in the cardiac outflow tract and atrioventricular canal, *Mech. Dev.* 106 (2001) 147–150.
- [8] H. Yamazaki, R. Nusse, Identification of DCAP, a drosophila homolog of a glucose transport regulatory complex, *Mech. Dev.* 119 (2002) 115–119.
- [9] V. Ribon, R. Herrera, B.K. Kay, A.R. Saltiel, A role for CAP, a novel, multifunctional Src homology 3 domain-containing protein in formation of actin stress fibers and focal adhesions, *J. Biol. Chem.* 273 (1998) 4073–4080.
- [10] N. Kioka, K. Ueda, T. Amachi, Vinexin, CAP/ponsin, ArgBP2: a novel adaptor protein family regulating cytoskeletal organization and signal transduction, *Cell Struct. Funct.* 27 (2002) 1–7.
- [11] K. Mandai, H. Nakanishi, A. Satoh, K. Takahashi, K. Satoh, H. Nishioka, A. Mizoguchi, Y. Takai, Ponsin/SH3P12: an I-Afadin- and vinculin-binding protein localized at cell–cell and cell–matrix adherens junctions, *J. Cell Biol.* 144 (1999) 1001–1018.
- [12] B. Wang, E.A. Golemis, G.D. Kruh, ArgBP2, a multiple Src homology 3 domain-containing, Arg/Abl-interacting protein, is phosphorylated in v-Abl-transformed cells and localized in stress fibers and cardiocyte Z-disks, *J. Biol. Chem.* 272 (1997) 17542–17550.
- [13] A. Suwa, M. Mitsushima, T. Ito, M. Akamatsu, K. Ueda, T. Amachi, N. Kioka, Vinexin beta regulates the anchorage dependence of ERK2 activation stimulated by epidermal growth factor, *J. Biol. Chem.* 277 (2002) 13053–13058.
- [14] J. Winkler, H. Lunsdorf, B.M. Jockusch, The ultrastructure of chicken gizzard vinculin as visualized by high-resolution electron microscopy, *J. Struct. Biol.* 116 (1996) 270–277.
- [15] C. Bakolitsa, J.M. de Pereda, C.R. Bagshaw, D.R. Critchley, R.C. Liddington, Crystal structure of the vinculin tail suggests a pathway for activation, *Cell* 99 (1999) 603–613.
- [16] R.P. Johnson, S.W. Craig, An intramolecular association between the head and tail domains of vinculin modulates talin binding, *J. Biol. Chem.* 269 (1994) 12611–12619.
- [17] R.P. Johnson, S.W. Craig, F-actin binding site masked by the intramolecular association of vinculin head and tail domains [see comments], *Nature* 373 (1995) 261–264.
- [18] M. Kroemker, A.H. Rudiger, B.M. Jockusch, M. Rudiger, Intramolecular interactions in vinculin control alpha-actinin binding to the vinculin head, *FEBS Lett.* 355 (1994) 259–262.
- [19] G.J. Miller, E.H. Ball, Conformational change in the vinculin C-terminal depends on a critical histidine residue (His-906), *J. Biol. Chem.* 276 (2001) 28829–28834.
- [20] G.J. Miller, S.D. Dunn, E.H. Ball, Interaction of the N- and C-terminal domains of vinculin. Characterization and mapping studies, *J. Biol. Chem.* 276 (2001) 11729–11734.
- [21] S. Huttelmaier, O. Mayboroda, B. Harbeck, T. Jarchau, B.M. Jockusch, M. Rudiger, The interaction of the cell-contact proteins VASP and vinculin is regulated by phosphatidylinositol-4,5-bisphosphate, *Curr. Biol.* 8 (1998) 479–488.
- [22] A.P. Gilmore, K. Burridge, Regulation of vinculin binding to talin and actin by phosphatidylinositol-4-5-bisphosphate, *Nature* 381 (1996) 531–535.
- [23] J. Weekes, S.T. Barry, D.R. Critchley, Acidic phospholipids inhibit the intramolecular association between the N- and C-terminal regions of vinculin, exposing actin-binding and protein kinase C phosphorylation sites, *Biochem. J.* 314 (1996) 827–832.
- [24] N.P. Brindle, M.R. Holt, J.E. Davies, C.J. Price, D.R. Critchley, The focal-adhesion vasodilator-stimulated phosphoprotein (VASP) binds to the proline-rich domain in vinculin, *Biochem. J.* 318 (Pt. 3) (1996) 753–757.
- [25] M. Reinhard, M. Rudiger, B.M. Jockusch, U. Walter, VASP interaction with vinculin: a recurring theme of interactions with proline-rich motifs, *FEBS Lett.* 399 (1996) 103–107.
- [26] K.A. DeMali, C.A. Barlow, K. Burridge, Recruitment of the Arp2/3 complex to vinculin: coupling membrane protrusion to matrix adhesion, *J. Cell Biol.* 159 (2002) 881–891.
- [27] C. Bakolitsa et al., Structural basis for vinculin activation at sites of cell adhesion, *Nature* 430 (2004) 583–586.
- [28] T. Izard, C. Vornrhein, Structural basis for amplifying vinculin activation by talin, *J. Biol. Chem.* 279 (2004) 27667–27678.
- [29] T. Izard, G. Evans, R.A. Borgon, C.L. Rush, G. Bricogne, P.R. Bois, Vinculin activation by talin through helical bundle conversion, *Nature* 427 (2004) 171–175.
- [30] R.A. Borgon, C. Vornrhein, G. Bricogne, P.R. Bois, T. Izard, Crystal structure of human vinculin, *Structure (Camb.)* 12 (2004) 1189–1197.
- [31] J.L. Rodriguez Fernandez, B. Geiger, D. Salomon, A. Ben-Ze'ev, Overexpression of vinculin suppresses cell motility in BALB/c 3T3 cells, *Cell Motil. Cytoskeleton* 22 (1992) 127–134.
- [32] B. Geiger, O. Ayalon, D. Ginsberg, T. Volberg, J.L. Rodriguez Fernandez, Y. Yarden, A. Ben-Ze'ev, Cytoplasmic control of cell adhesion, *Cold Spring Harb. Symp. Quant. Biol.* 57 (1992) 631–642.
- [33] W.H. Goldmann, M. Schindl, T.J. Cardozo, R.M. Ezzell, Motility of vinculin-deficient F9 embryonic carcinoma cells analyzed by video, laser confocal, and reflection interference contrast microscopy, *Exp. Cell Res.* 221 (1995) 311–319.
- [34] W. Xu, H. Baribault, E.D. Adamson, Vinculin knockout results in heart and brain defects during embryonic development, *Development* 125 (1998) 327–337.
- [35] W. Xu, J.L. Coll, E.D. Adamson, Rescue of the mutant phenotype by reexpression of full-length vinculin in null F9 cells; effects on cell

- locomotion by domain deleted vinculin, *J. Cell Sci.* 111 (Pt. 11) (1998) 1535–1544.
- [36] J.L. Coll, A. Ben-Ze'ev, R.M. Ezzell, J.L. Rodriguez Fernandez, H. Baribault, R.G. Oshima, E.D. Adamson, Targeted disruption of vinculin genes in F9 and embryonic stem cells changes cell morphology, adhesion, and locomotion, *Proc. Natl. Acad. Sci. USA* 92 (1995) 9161–9165.
- [37] J.L. Rodriguez Fernandez, B. Geiger, D. Salomon, A. Ben-Ze'ev, Suppression of vinculin expression by antisense transfection confers changes in cell morphology, motility, and anchorage-dependent growth of 3T3 cells, *J. Cell Biol.* 122 (1993) 1285–1294.
- [38] J.L. Rodriguez Fernandez, B. Geiger, D. Salomon, I. Sabanay, M. Zoller, A. Ben-Ze'ev, Suppression of tumorigenicity in transformed cells after transfection with vinculin cDNA, *J. Cell Biol.* 119 (1992) 427–438.
- [39] M.C. Subauste, O. Pertz, E.D. Adamson, C.E. Turner, S. Junger, K.M. Hahn, Vinculin modulation of paxillin-FAK interactions regulates ERK to control survival and motility, *J. Cell Biol.* 165 (2004) 371–381.
- [40] R.R. Evans, R.M. Robson, M.H. Stromer, Properties of smooth muscle vinculin, *J. Biol. Chem.* 259 (1984) 3916–3924.
- [41] M. Wakabayashi, T. Ito, M. Mitsushima, S. Aizawa, K. Ueda, T. Amachi, N. Kioka, Interaction of lp-dlg/KIAA0583, a membrane-associated guanylate kinase family protein, with vinexin and beta-catenin at sites of cell–cell contact, *J. Biol. Chem.* 278 (2003) 21709–21714.
- [42] H. Chen, D.M. Cohen, B. Choudhury, N. Kioka, E.D. Adamson, S.W. Craig, Spatial distribution and functional significance of activated vinculin in living cells, *J. Cell Biol.* 169 (2005) 459–470.